3rd European supercritical CO_2 Conference
September 19-20, 2019, Paris, France

2019-sCO_2.eu-133

MODELLING AND PERFORMANCE ANALYSIS OF A SUPERCRITICAL CO_2 SYSTEM FOR HIGH TEMPERATURE INDUSTRIAL HEAT TO POWER CONVERSION AT OFF-DESIGN CONDITIONS

Matteo Marchionni
Brunel University London
Uxbridge, United Kingdom

Samira S. Saravi
Brunel University London
Uxbridge, United Kingdom

Giuseppe Bianchi *
Brunel University London
Uxbridge, United Kingdom
Email: giuseppe.bianchi@brunel.ac.uk

Savvas A. Tassou
Brunel University London
Uxbridge, United Kingdom

ABSTRACT

Industrial processes are currently characterized by thermal energy losses through high temperature exhausts or effluents (above 300°C) that, on a global scale, account for nearly 11.4% of their primary energy consumption, namely 12.1 EJ. For these high temperature exhausts, conventional waste heat to power conversion systems based on bottoming thermodynamic cycles are not very suitable since most of the state of the art working fluids are not able to perform safely and efficiently at high temperatures. Supercritical Carbon Dioxide (sCO_2) power systems allow to overcome these limitations because of the chemical and thermo-physical properties of the working fluid.

In order to provide insights on the behavior of sCO_2 systems, this paper presents the development of a one-dimensional numerical model of a low capacity (50 kW_e) simple regenerated system for medium to high temperature waste heat recovery applications. The unit is equipped with single-shaft radial turbomachinery and different heat exchanger technologies such as micro-tube, printed circuit, plate, etc. Flue gas and water are used as heat source and sink respectively. At nominal conditions, i.e. for a flue gas mass flow rate of 1.0 kg/s at 650°C, the unit operates at a cycle pressure ratio of 1.7, generating 50 kW_e with a thermal efficiency of 20%. The paper first discusses the modelling methodology, including turbomachinery and heat exchanger models implementation, and then assesses the steady-state performance of the unit at design and off-design operating conditions. From the simulations carried out operating maps of the unit have been obtained to form the baseline for the setting up of control strategies for the sCO_2 system. The results show that the system can generate up to 75 kWe for a heat source mass flow rate of 1.2 kg/s and heat source temperature of 700°C.

INTRODUCTION

The increasing energy demand and the environmental concerns posed by the extensive use of fossil fuel, have steered research interest towards more sustainable power generation. In this context, a major challenge is the significant amount of thermal energy losses occurring in industrial processes. Indeed, on global scale, almost 30% of the primary energy consumption is rejected, through exhausts or effluents, into the environment [1]. To efficiently recover and re-use this thermal energy, heat to power conversion systems based on bottoming thermodynamic cycles represent one of the most promising technologies. Unlike those applications rejecting heat at low temperatures which benefit from commercially available solutions like the Organic Rankine Cycle (ORC) systems [2], the exploitation of exhausts and effluents at temperatures higher than 300°C still represents a technical challenge.

A promising technology for such applications is the Joule-Brayton cycle, using supercritical CO_2 (sCO_2) as working fluid, which allows to achieve higher efficiencies than ORCs due to the advantageous thermo-physical properties of the CO_2 near the critical point [3,4]. Many works are available in the literature on sCO_2 heat to power conversion systems. Theoretical investigations have been presented in references [5–8] to assess how different cycle architectures could improve system performance and economic figures. Numerical and experimental studies have also been performed on individual unit components such as heat exchangers, turbomachines and auxiliaries to overcome the technical challenges arising when CO_2 is used as a working fluid.

Kwon et al. [9] and Fu et al. [10] presented different numerical models of Printed Circuit Heat Exchangers (PCHEs) to predict their off-design behavior when used as gas cooler or recuperator in sCO_2 Brayton power cycles, while Bae et al. [11]

* corresponding author(s)

DOI: 10.17185/duepublico/48908

proposed a new set of heat transfer and pressure drop correlations for these heat exchangers.

Several studies have also been carried out on sCO_2 turbomachinery. Various design methodologies have been developed for turbines [12,13], compressors [14–17] and auxiliaries such as bearings and seals [18,19], which in sCO_2 applications are of paramount importance to prevent leakage and to guarantee lubrication at high pressures and revolution speeds. Several computational models have also been implemented to predict their off-design performance [20-22], but few experimental analyses can be found. Experimental compressor and turbine performance maps have been presented only by Wright et al. [23], while experimental investigations of centrifugal compressors close to the CO_2 critical point have been reported by Utamura et al. [24] and Fuller and Eisemann [25].

Despite the intensive research from a purely theoretical point of view and from a component wise perspective, few works are available on the overall performance of small-scale power units (50-100 kWe), particularly at off design conditions.

Lambruschini et al. [26] developed a model in Matlab Simulink of a 10 MW_e recompression Brayton cycle for power generation applications. Performance maps were used to predict the behaviour of turbomachines, while simple models (i.e. fixed heat transfer coefficient) were considered for the heat exchangers. Even though the dynamics of the system were investigated, more complex models are needed for heat exchangers in order to accurately predict the behaviour of the unit also in operating conditions far from the design point. A more detailed model developed in Dymola has been proposed by Zhang et al. in [27]. Performance maps were used to model the turbomachines while for the heat exchangers a finite volume approach was adopted. In particular, the local heat transfer coefficient for different operating conditions of the heat exchangers was predicted using heat transfer correlations. However, the heat exchanger models did not take into account the different heat exchanger technologies employed. Similarly, Luu et al. in [28] developed a model of a high capacity sCO_2 recompression cycle system for Concentrated Solar Power applications. Also in this work, the same approach has been used to model all the system heat exchangers, independently from the technology used.

The models reported in the literature not only refer to high capacity power units but also to layouts and component technologies that are specific to solar or nuclear power applications. In system models, heat exchangers are modelled independently from their typology and their specific geometrical and technological features. These assumptions may affect the validity of the overall performance predictions.

To fill the gap in the literature, in this work a more detailed model of a low capacity sCO_2 heat to power conversion system has been developed. The sCO_2 unit has been designed for Waste Heat Recovery (WHR) applications and therefore considers a simple regenerated layout due to its lower complexity and investment cost. The model implements performance maps for the turbomachines while each different heat exchanger is modelled considering its geometrical features and using manufacturer's data for calibration. The system performance has been investigated at design and off-design conditions. Amongst the main outputs, are performance maps for the whole system which can be used for control design purposes.

MODELLING METHODOLOGY

The model presented in this work refers to a 50 kW_e sCO_2 simple regenerated Brayton cycle unit for medium to high thermal grade WHR applications under construction at Brunel University London [29]. The facility employs flue gases as heat source and water as heat sink, either if other cooling sources can be used (i.e. air coolers). Both compressor and turbine are centrifugal machines, while plate, printed circuit and micro-tube heat exchangers are considered for the gas cooler, the recuperator and the primary heater respectively.

The model of the system has been developed in the commercial software platform GT-SUITE™. Figure 1 shows the model block diagram, where the uppercase captions point to the sub-models of each component, while the lowercase ones refer to the boundary and initial conditions of the model.

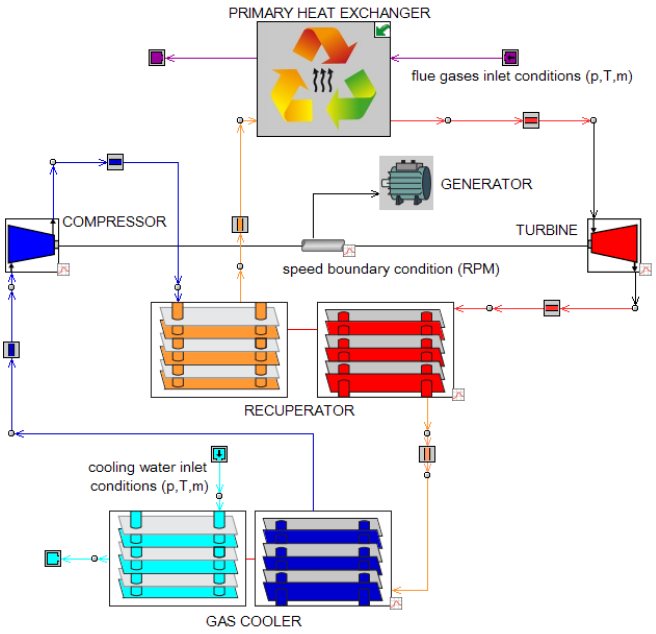

Figure 1: sCO_2 system model developed in GT-SUITE™.

The heat exchangers are modelled following a one-dimensional approach. According to their geometrical features, the hot and cold sides of the heat exchangers are approximated as one-dimensional (1-D) channels with an equivalent length and cross-sectional area. Both sides are therefore interconnected through convective connections to a thermal mass, which accounts for the thermal inertia of the heat exchanger and considers its real material properties. To account of the thermo-fluid property change, the channels and the thermal mass are discretized along the flow direction in a certain number of sub-volumes. Consequently, following the so called 'staggered grid approach' [30], the 1-D Navier-Stokes equations are numerically

DOI: 10.17185/duepublico/48908

solved to calculate the mass flow rates, pressures and total enthalpies of the hot and cold flows at the boundaries of the channels' sub-volumes. The other thermodynamic scalar quantities are computed through a dynamic-link library of the NIST Refprop database [31] and assumed constant in the whole sub-volume domain.

In order to solve the energy equation, the computation of the local heat transfer coefficients between the heat exchanger walls and the cold and hot channels respectively is required. For the refrigerant side (sCO_2 flow), the Gnieliski heat transfer correlation is employed [32] and calibrated against performance data provided by the manufacturers. For the non-refrigerant one (i.e. water or air), these data are used to calculate the best fitting coefficients of the Nusselt-Reynolds (Nu-Re) correlations for the equivalent 1-D networks. These correlations are then adopted to calculate the heat transfer coefficients [33].

Manufacturer data provide performance characteristics for different flow rates of the two working fluids to span a wide range of Reynolds numbers. This allows the prediction of the heat exchanger performance at off-design conditions. The pressure drops across the heat exchanger are computed using a modified version of the Colebrook equation [34]. A more detailed description of the modelling methodology can be found in [35,36].

The same modelling approach has been employed for the pipes connecting the different components, with the only difference that thermal losses are neglected. The inertia due to the mechanical shaft connecting the turbomachines and that of the generator are taken into account. Parasitic losses of the system ancillaries, such as the water cooling pump and the compressors required to extract the leakage flows from the generator cavity, have not been considered for the calculation of the system performance.

INTEGRATION OF TURBOMACHINERY MAPS

For the modelling of the turbomachines, performance maps have been used, generated by using three-dimensional Computational Fluid Dynamic (CFD) models. The compressor and turbine impeller geometries selected during the design stage are similar to the ones tested at the Sandia sCO_2 compression loop facility [23]. The number of vanes are equal (6+6, as shown in Figure 2) but the blade shape has been modified and the wheels dimensions scaled to achieve a higher efficiency. A wheel diameter of 57.12 mm has been selected for the turbine and 44.03 mm for the compressor. For the design and model of the turbomachines, different packages in ANSYS have been used (i.e. CCD, RTD and BladeGen).

To perform validation of the model, simulations have been carried out assuming the initial thermodynamic conditions of the CO_2 to be in the supercritical region. The inlet temperature has been set equal to 32.5°C, the inlet pressure 78.7 bar, and the design shaft speed has been set at 55,000 RPM. Compressor inlet operating conditions were determined to avoid the formation of liquid where the flow is accelerated locally.

ANSYS CFX 17.1 was employed to perform single-passage steady state calculations. The wheel's mesh has been generated in ANSYS-TurboGrid, shown in Figure 2, together with the flow path of the compressor. An Automatic Topology and Meshing feature (ATM optimized) has been employed inside the impeller, with a mesh of approximately 10^{+6} nodes (Figure 2). The k-ε and total energy models have been used to take into account the flow turbulence and its compressibility, with total pressure and total temperature defined as inlet boundary conditions and the flow direction considered normal to the boundary. Outlet average static pressure has been chosen as outlet boundary condition.

Figure 2: ANSYS-TurboGrid Mesh and flow path for Supercritical CO_2 compressor.

To simulate the real gas effect, the Span-Wagner Equation of State model has been used to accurately generate the flow properties [37]. For this purpose, a Real Gas Property (RGP) format table has been created to implement the variable properties in the CFX code. The user-defined table includes CO_2 features such as specific heat ratio and density near the critical point, which fluctuates due to the phase change effect. These features have been created using the NIST Refrop 8.0 fluid property database. The generated property files have been combined with a MATLAB code to create a lookup table as an input of TASCflow RGP in ANSYS CFX 17.1.

Once validated, the model results have been used to obtain the turbomachinery performance data, which have been employed to generate the turbine and compressor performance maps in GT-SUITE™.

Figures 3 and 4 show the compressor operating and efficiency maps respectively. The maps are expressed in reduced data, meaning that the mass flow rate and revolution speed are scaled with the reference pressure and temperature considered to generate the data. Figure 5 and Figure 6 show instead the operating and efficiency maps of the turbine.

Each of these maps has been generated by maintaining constant the inlet thermodynamic conditions of the working fluid (pressure and temperature) and changing the outlet static pressure at different revolution speeds (at least five pressure ratios for each revolution speed are required to ensure an accurate interpolation of the operating curves). Beyond the speed range of the simulated working points, a linear extrapolation method is used to predict the performance of the turbomachines.

A small distortion is noticeable in these maps, which is particularly located in the surge line. This is due to the change in the pressure rise characteristics occurring between higher and lower rotational speeds. The pressure changes inside the

DOI: 10.17185/duepublico/48908

compressor stages for different speeds have been influenced by the supercritical CO_2 characteristics.

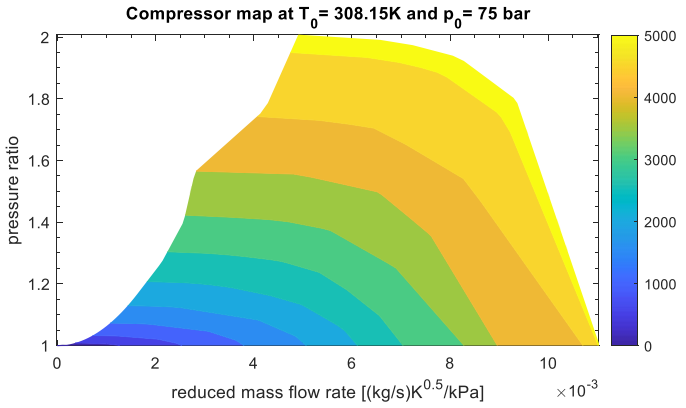

Figure 3: Compressor operating map generated for a reference temperature and pressure of 308.15K and 75 bar respectively (revolution speed expressed in reduced RPM [RPM/$K^{0.5}$]).

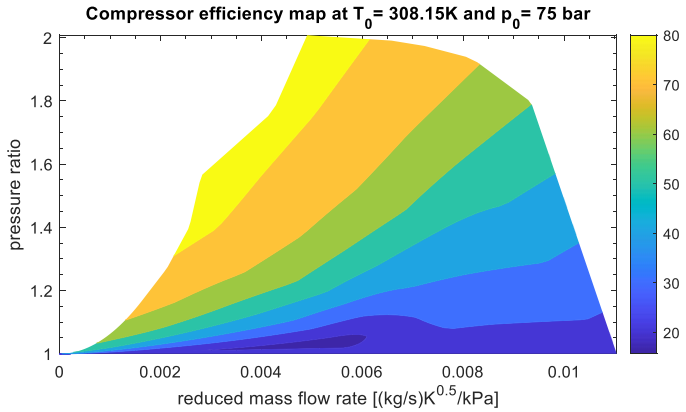

Figure 4: Compressor efficiency map generated for a reference temperature and pressure of 308.15K and 75 bar respectively (efficiency expressed in percentage units [%]).

The operation target for this compressor in the supercritical region approaches the critical point. This condition has positive effect on the choke line. In fact, the real gas properties of the CO_2 lead to a reduction of the choke margin in the compressor stage compared to the one typical of conventional machines using ideal gases [37].

RESULTS AND DISCUSSION

After the model validation stage, a series of simulations have been carried out to assess the steady-state performance of the sCO_2 system. The heat source and heat sink mass flow rates and inlet temperatures have been varied to analyze their effect on the unit, the net power output and thermal efficiency as well as on the temperature of the working fluid at the inlet of the turbine and the compressor, which are of important relevance to the cycle performance [8]. The revolution speed of the turbomachines has been maintained constant and equal to the design point for the whole set of simulations. Tables 1 and 2 summarize the nominal operating conditions of the system at the design point as well as the input and output quantities of the model.

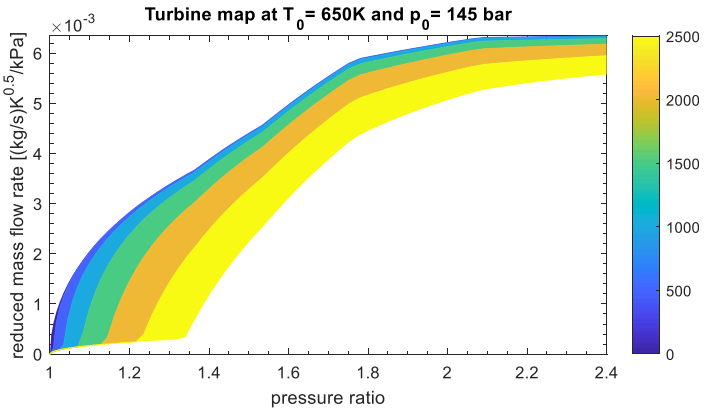

Figure 5: Turbine operating map generated for a reference temperature and pressure of 650K and 145 bar respectively (revolution speed expressed in reduced RPM [RPM/$K^{0.5}$]).

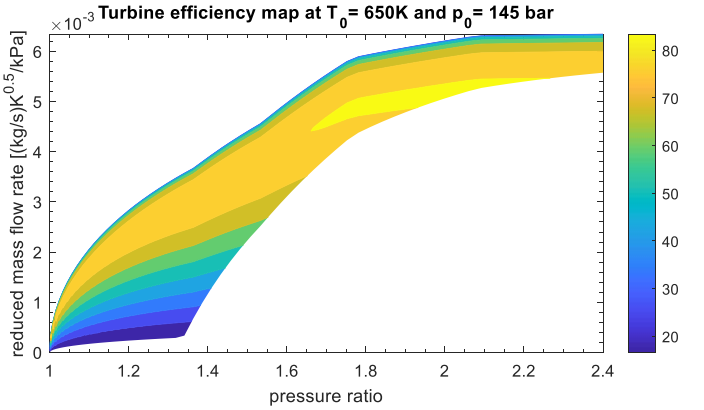

Figure 6: Turbine efficiency map generated for a reference temperature and pressure of 650K and 145 bar respectively (efficiency expressed in percentage units [%]).

Table 1 – Operating conditions of the sCO_2 unit at the design point

Supercritical CO_2		Design	Model I/O
Mass flow rate	[kg/s]	2.1	Output
Highest pressure	[bar]	128	Output
Lowest pressure	[bar]	75	Output
Heat source: flue gas			
Mass flow rate	[kg/s]	1.0	Input
Inlet temperature	[°C]	650	Input
Inlet pressure	[bar]	1	Input
Cold source: Water			
Mass flow rate	[kg/s]	1.6	Input
Inlet temperature	[°C]	25	Input
Inlet pressure	[bar]	3	Input

DOI: 10.17185/duepublico/48908

Table 2 – Turbomachinery operating conditions at the design point

Compressor		Design	Model I/O
Revolution speed	[RPM]	86000	Input
Isentropic efficiency	[%]	75	Output
Inlet temperature	[°C]	36	Output
Turbine			
Revolution speed	[RPM]	86000	Input
Isentropic efficiency	[%]	80	Output
Inlet temperature	[°C]	400	Output
sCO_2 unit			
Mechanical net power output	[kW]	50	Output
Overall efficiency	[%]	20	Output

Figure 7 shows how the power output of the sCO_2 unit changes following the variations of the heat load, namely the inlet temperature and mass flow rate. In this set of simulations, the inlet conditions of the heat sink have been maintained constant and equal to the design values. The cycle pressure ratio slightly changes depending on the heat load supplied at the heater. In particular, it can be seen that the map gives an indication of the limit conditions of the waste heat source for which the sCO_2 system is not able to generate power. It can be observed that for flue gas mass flow rates lower than 0.8 kg/s, the inlet temperature of the heat exchanger must be higher than 500°C in order to have a not null net power output. For lower temperatures, the compressor requires more power than the one generated by the turbine and consequently the net power output of the system is negative, around -15 kW (Figure 7). This is mainly due to the low design pressure ratio of the cycle, which together with the low divergence of the CO_2 isobaric lines, requires the achievement of high turbine inlet temperatures to reach a positive power output.

For this reason, high exhaust temperatures are needed to achieve high system power outputs. For instance, for a unitary exhaust mass flow rate, considering a flue gas temperature increase from 600°C to 850°C, the unit power output rises from 45 kW to 90 kW. If the same percentage change in the hot source mass flow rate occurs, for example at 650°C, the net outcome varies only from 50 kW to 62 kW.

The increase of the hot source mass flow rate, only leads to a slightly higher working fluid mass flow rate in the circuit to balance the higher thermal load available at the primary heater. Consequently, the thermal efficiency of the system remains almost constant and the power output gain is achieved thanks to the greater mass flow rate of CO_2 processed. On the contrary, a rise of the hot source temperature leads to a higher working fluid temperature at the turbine inlet, with a positive effect on the cycle thermal efficiency.

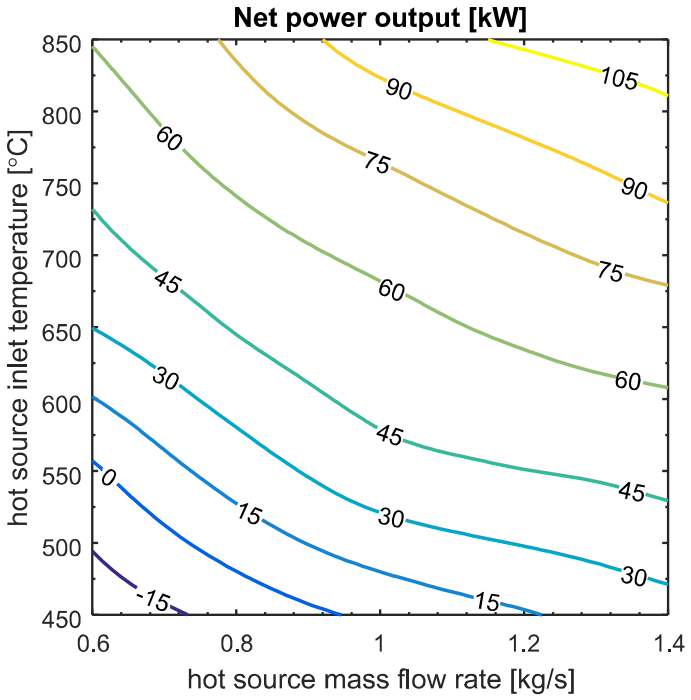

Figure 7: sCO_2 unit net power output as a function of the heat source inlet temperature and mass flow rate

Figure 8 confirms the abovementioned statement, showing a higher sensitivity of the cycle thermal efficiency to the hot source inlet temperature rather than its mass flow rate. In fact, a variation of the latter quantity from 0.8 kg/s to 1.2 kg/s at 650°C, leads to an efficiency rise of almost 12% (from 16% to 18%), against a 52% increase (from 10% to 22%) for the same percentage change of flue gas temperature (considering a 1.0 kg/s mass flow rate). An even higher efficiency (around 30%) can be achieved for an exhaust temperature of 850°C and a mass flow rate of 1.4 kg/s. A further increased efficiency can be obtained by increasing the design cycle pressure ratio, which would lead however to increased investment and operational costs due to higher-end materials and more expensive components, which is not desirable for WHR applications.

The efficiency of the cycle is also strongly influenced by the sCO_2 temperature at the turbine inlet. For the design adopted, the highest system power output and efficiency occur when a temperature at the turbine inlet of 650°C is reached (Figure 9). and are equal to 105 kW (Figure 7) and 30% (Figure 8) respectively.

For turbine inlet temperature lower than 275°C, occurring for a hot source mass flow rate and inlet temperature lower than 0.9 kg/s and 550°C respectively (Figure 9), the system is not able to generate net power output (Figure 7).

DOI: 10.17185/duepublico/48908

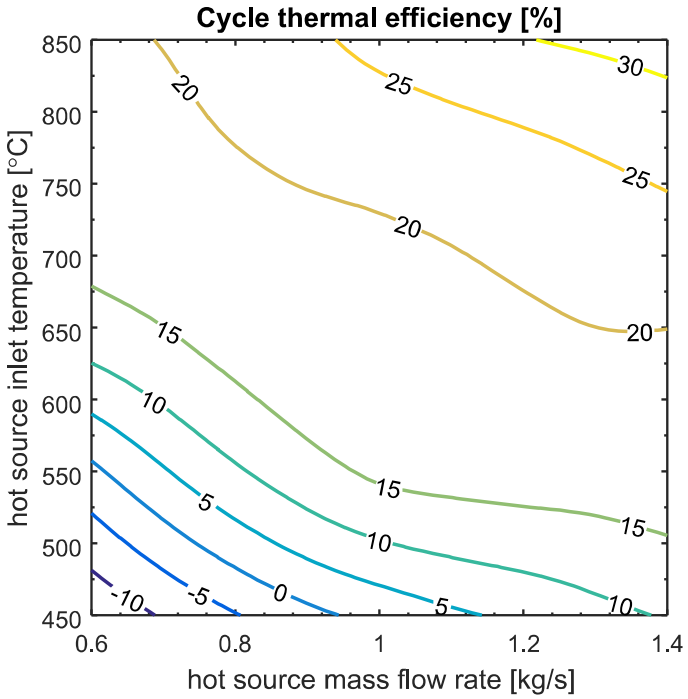

Figure 8: Variation of sCO_2 unit thermal efficiency with heat source inlet temperature and mass flow rate.

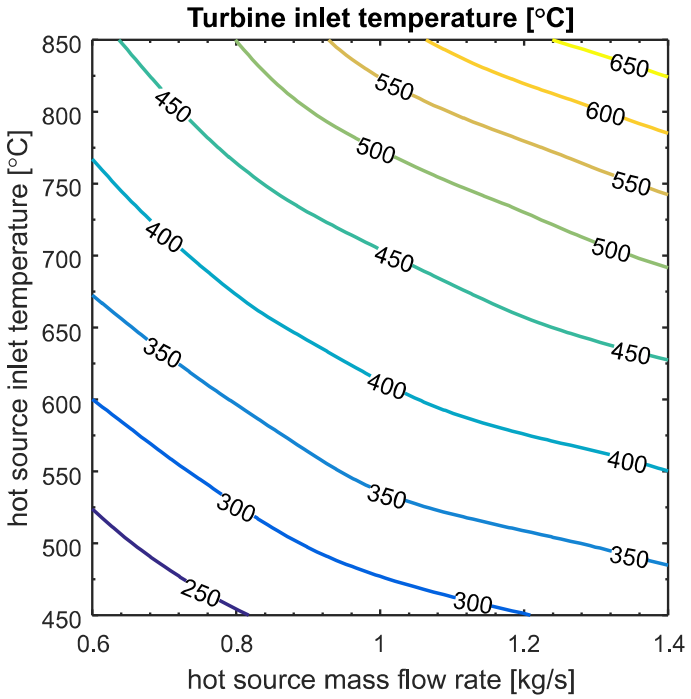

Figure 9: Variation of sCO_2 temperature at the turbine inlet with heat source inlet temperature and mass flow rate.

In particular, the results shown in Figure 9 suggest that it is possible to reduce the relevant temperature difference between the inlet temperature of the flue gases and the CO_2 at the turbine inlet by increasing the flue gas mass flow rate. For instance, if a hot source inlet temperature of 650°C is considered, increasing the hot source mass flow rate from 1 kg/s up to 1.4 kg/s can lead to a rise in the turbine inlet temperature from 400°C to 450°C, with a consequent increase in the power output from 50 kW to 63 kW (Figure 7) and of the thermal efficiency from 17% to almost 20% (Figure 8).

This increase in performance is due to the lower exergy loss occurring in the primary heater. Increasing the mass flow rate of the hot source counterbalances the higher thermal capacity of the CO_2. Then, a better matching of the temperature profiles of the two fluids in the heat exchanger can be achieved, leading to a higher exergy efficiency. A further solution would be the adoption of different cycle layouts designed to achieve better temperature profile matching. However, the higher investment cost due to the additional components required (i.e. heat exchangers, compressors and turbines), may increase the payback period of the heat to power conversion unit disproportionally.

A further positive effect on the system performance can also be achieved by reducing the inlet temperature of the cold source, as showed in Figure 10. Given a cooling fluid mass flow rate of 1.6 kg/s, a reduction of 20% in its inlet temperature can actually lead to a power output increase from 48 kW to 64 kW. Similarly, the same percentage variation of cold source mass flow rate, at an inlet temperature of 18°C, allows an increase in the system power output from 54 kW to 64 kW.

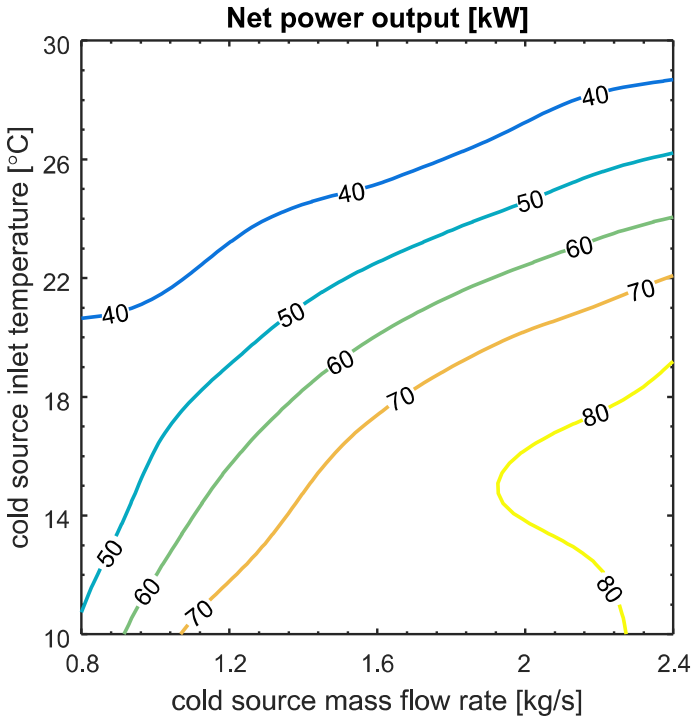

Figure 10: Variation of sCO_2 unit net power output with cold source inlet temperature and mass flow rate.

In particular, an increase of the cooling load allows to decrease the compressor inlet temperature of the CO_2, which gets closer to the critical point. At critical conditions, the CO_2

DOI: 10.17185/duepublico/48908

isothermal compressibility increases steeply, allowing a more efficient compression. The decreased compression power then leads to an increased system net power output and thermal efficiency.

The thermal efficiency gain achievable is shown in Figure 11. Considering a a cold source mass flow rate of 1.6 kg/s, a decrease of its inlet temperature from 26°C down to 16°C leads to an increase in the cycle thermal efficiency from 9% to 21%. A higher efficiency value of 24% can be reached by increasing the cooling flow rate to 2.4 kg/s, and keeping its inlet temperature lower than 18°C. For higher cooling fluid temperatures the maximum efficiency is limited to 20%.

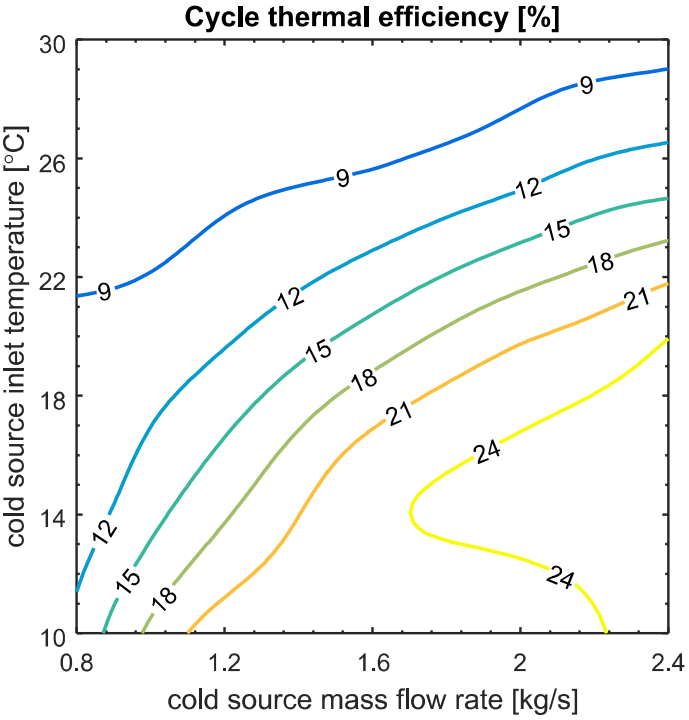

Figure 11: Variation of sCO_2 unit thermal efficiency with cold source inlet temperature and mass flow rate.

It can also be seen from Figures 10 and 11, that for mass flow rates higher than 1.6 kg/s and inlet temperatures lower than 20°C, less steep performance improvements can be observed. Considering for instance a cold source inlet temperature of 14°C and a variation of mass flow rate from 1.6 kg/s to 2.4 kg/s (Figure 10), the system power output increases only from 75 kW to 80 kW and the thermal efficiency from 23% to 24% (Figure 11).

The reason for this can be explained by referring to Figure 12, which shows the variation in the CO_2 temperature at the compressors inlet as a function of the cooling load available at the gas cooler. In the range of cold source inlet conditions considered, the compressor inlet temperature is constant and equal to 35°C. No further temperature reductions could be achieved even for increased cooling flow rate, due to the higher thermal capacity that the CO_2 assumes close to the critical point. This ensures a CO_2 temperature at the compressor inlet always higher than the critical temperature which avoids condensation and dry conditions at the start of compression.

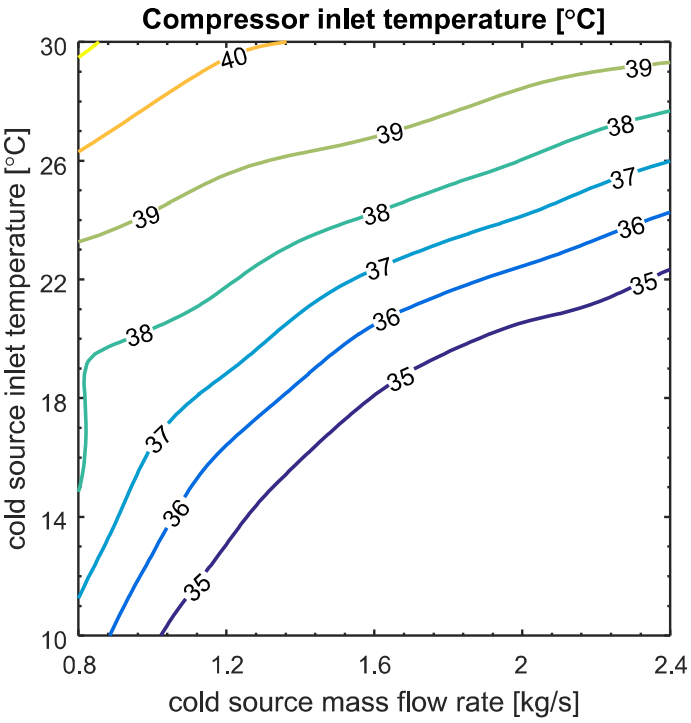

Figure 12: Variation of sCO_2 temperature at the compressor inlet with cold source inlet temperature and mass flow rate.

CONCLUSIONS

The aim of the research presented in this paper was to investigate the off-design performance of a low capacity sCO_2 heat to power conversion unit designed for medium to high thermal grade WHR applications. To model each component, performance data provided by manufacturers or obtained from more complex CFD models have been used. In particular, the operating maps of the radial compressor and turbine have been generated and presented.

Off-design steady state simulations were carried out to assess the effect of the hot and cold source inlet conditions on the unit performance as well as on the sCO_2 temperature at the inlet of the compressor and turbine. Performance maps of the sCO_2 unit have been generated and can be used in the design of control strategies for the system. In particular, the maps showed that the unit is not able to generate power if a heat source mass flow of 0.8 kg/s is used at a temperature lower than 500°C, due to the low sCO_2 temperature at the turbine inlet (275°C).

The temperature of the cold sink can have a significant influence on the unit power output and efficiency. For a fixed heat load and assuming a coolant mass flow rate of 1.6 kg/s, a decrease in the cooling fluid inlet temperature from 26°C to 16°C leads to an increase in the system power output and efficiency from 40 kW to 72 kW and from 9% up to 21% respectively, Moreover, the analysis showed that no condensation at the

DOI: 10.17185/duepublico/48908

compressor inlet occurs since the minimum temperature achieved is 35°C, which ensures safe operating conditions for the compressor over the whole range of cooling fluid inlet temperatures investigated.

NOMENCLATURE

CFD	Computational Fluid Dynamics
I/O	Input/Output
p_0	Reference pressure
RPM	Revolutions Per Minute
sCO_2	supercritical carbon dioxide
T_0	Reference temperature
WHR	Waste Heat Recovery

ACKNOWLEDGEMENTS

Aspects of the work have been funded by: i) European Union's Horizon 2020 research and innovation program under grant agreement No. 680599; ii) the Centre for Sustainable Energy Use in Food Chains (CSEF) of Brunel University London. CSEF is an End Use Energy Demand Centre funded by the Research Councils UK, Grant No: EP/K011820/1 and EPSRC project OPTEMIN (Optimising Energy Management in Industry) Grant No. EP/P004636/1. The authors would like to acknowledge the funders as well as contributions from Mr. Jonathan Harrison of Gamma Technologies during the model development. The paper all relevant data to support the understanding of the results. More detailed information and data, if required, can be obtained by contacting the corresponding author of the paper.

REFERENCES

[1] Forman C, Muritala IK, Pardemann R, Meyer B. Estimating the global waste heat potential. Renewable and Sustainable Energy Reviews 2016;57:1568–79. doi:10.1016/J.RSER.2015.12.192.

[2] Tchanche BF, Lambrinos G, Frangoudakis A, Papadakis G. Low-grade heat conversion into power using organic Rankine cycles – A review of various applications. Renewable and Sustainable Energy Reviews 2011;15:3963–79. doi:10.1016/j.rser.2011.07.024.

[3] Freund P, Bachu S, Simbeck D, Thambimuthu K. Annex I: Properties of CO 2 and carbon-based fuels. IPCC Special Report on 2005.

[4] Dostal V, Driscoll M, Hejzlar P. A supercritical carbon dioxide cycle for next generation nuclear reactors 2004.

[5] Turchi CS, Ma Z, Neises TW, Wagner MJ. Thermodynamic Study of Advanced Supercritical Carbon Dioxide Power Cycles for Concentrating Solar Power Systems. Journal of Solar Energy Engineering 2013;135:41007. doi:10.1115/1.4024030.

[6] Manjunath K, Sharma OP, Tyagi SK, Kaushik SC. Thermodynamic analysis of a supercritical/transcritical CO2 based waste heat recovery cycle for shipboard power and cooling applications. Energy Conversion and Management 2018;155:262–75. doi:10.1016/j.enconman.2017.10.097.

[7] Kulhánek M, Dostál V. Supercritical Carbon Dioxide Cycles Thermodynamic Analysis and Comparison. Proceedings of SCCO2 Power Cycle Symposium 2011:1–12.

[8] Marchionni M, Bianchi G, Tassou SA. Techno-economic assessment of Joule-Brayton cycle architectures for heat to power conversion from high-grade heat sources using CO2 in the supercritical state. Energy 2018;148:1140–52. doi:10.1016/J.ENERGY.2018.02.005.

[9] Kwon JS, Bae SJ, Heo JY, Lee JI. Development of accelerated PCHE off-design performance model for optimizing power system operation strategies in S-CO2 Brayton cycle. Applied Thermal Engineering 2019;159:113845. doi:10.1016/J.APPLTHERMALENG.2019.113845.

[10] Fu Q, Ding J, Lao J, Wang W, Lu J. Thermal-hydraulic performance of printed circuit heat exchanger with supercritical carbon dioxide airfoil fin passage and molten salt straight passage. Applied Energy 2019;247:594–604. doi:10.1016/J.APENERGY.2019.04.049.

[11] Bae SJ, Kwon J, Kim SG, Son I, Lee JI. Condensation heat transfer and multi-phase pressure drop of CO2 near the critical point in a printed circuit heat exchanger. International Journal of Heat and Mass Transfer 2019;129:1206–21. doi:10.1016/J.IJHEATMASSTRANSFER.2018.10.055.

[12] Shin H, Cho J, Baik Y-J, Cho J, Roh C, Ra H-S, et al. Partial Admission, Axial Impulse Type Turbine Design and Partial Admission Radial Turbine Test for SCO2 Cycle. Volume 9: Oil and Gas Applications; Supercritical CO2 Power Cycles; Wind Energy, ASME; 2017, p. V009T38A019. doi:10.1115/GT2017-64349.

[13] Taehan Kigye Hakhoe., 대한 기계 학회. Taehan Kigye Hakhoe nonmunjip. B = B Transactions of the Korean Society of Mechanical Engineers. Taehan Kigye Hakhoe; 1996.

[14] Pelton R, Allison T, Jung S, Smith N. Design of a Wide-Range Centrifugal Compressor Stage for Supercritical CO2 Power Cycles. Volume 9: Oil and Gas Applications; Supercritical CO2 Power Cycles; Wind Energy, ASME; 2017, p. V009T38A031. doi:10.1115/GT2017-65172.

[15] Shao W, Wang X, Yang J, Liu H, Huang Z. Design Parameters Exploration for Supercritical CO2 Centrifugal Compressors Under Multiple Constraints. Volume 9: Oil and Gas Applications; Supercritical CO2 Power Cycles; Wind Energy, ASME; 2016, p. V009T36A008. doi:10.1115/GT2016-56820.

[16] Monje B, Sánchez D, Savill M, Pilidis P, Sánchez T. A Design Strategy for Supercritical CO2 Compressors. Volume 3B: Oil and Gas Applications; Organic Rankine Cycle Power Systems; Supercritical CO2 Power Cycles; Wind Energy, ASME; 2014, p. V03BT36A003. doi:10.1115/GT2014-25151.

[17] Pasch J, Stapp D. Testing of a New Turbocompressor for Supercritical Carbon Dioxide Closed Brayton Cycles. Volume 9: Oil and Gas Applications; Supercritical CO2 Power Cycles; Wind Energy, ASME; 2018, p. V009T38A024. doi:10.1115/GT2018-77044.

[18] Bidkar RA, Sevincer E, Wang J, Thatte AM, Mann A, Peter M, et al. Low-Leakage Shaft-End Seals for Utility-Scale Supercritical CO_2 Turboexpanders. Journal of Engineering for Gas Turbines and Power 2016;139:22503. doi:10.1115/1.4034258.

DOI: 10.17185/duepublico/48908

[19] Du Q, Gao K, Zhang D, Xie Y. Effects of grooved ring rotation and working fluid on the performance of dry gas seal. International Journal of Heat and Mass Transfer 2018;126:1323–32. doi:10.1016/J.IJHEATMASSTRANSFER.2018.05.055.

[20] Jeong WS, Kim TW, Suh KY. Computational Fluid Dynamics of Supercritical Carbon Dioxide Turbine for Brayton Thermodynamic Cycle. Volume 2: Fuel Cycle and High Level Waste Management; Computational Fluid Dynamics, Neutronics Methods and Coupled Codes; Student Paper Competition, ASME; 2008, p. 265–9. doi:10.1115/ICONE16-48240.

[21] Saravi SS. An investigation into sCO2 compressor performance prediction in the supercritical region for power systems. Energy Procedia 2019;161:403–11. doi:10.1016/J.EGYPRO.2019.02.098.

[22] Pecnik R, Rinaldi E, Colonna P. Computational Fluid Dynamics of a Radial Compressor Operating With Supercritical CO $_2$. Journal of Engineering for Gas Turbines and Power 2012;134:122301. doi:10.1115/1.4007196.

[23] Wright SA, Radel RF, Vernon ME, Rochau GE, Pickard PS. SANDIA REPORT Operation and Analysis of a Supercritical CO 2 Brayton Cycle. n.d.

[24] Utamura M, Fukuda T, Aritomi M. Aerodynamic Characteristics of a Centrifugal Compressor Working in Supercritical Carbon Dioxide. Energy Procedia 2012;14:1149–55. doi:10.1016/J.EGYPRO.2011.12.1068.

[25] Fuller, Robert L, Eisemann K. Centrifugal Compressor Off-design performance for supercritical CO2. Supercritical CO2 Power Cycle Symposium, Boulder, Colorado: 2011, p. 12.

[26] Lambruschini F, Liese E, Zitney SE, Traverso A. Dynamic Model of a 10 MW Supercritical CO $_2$ Recompression Brayton Cycle. Volume 9: Oil and Gas Applications; Supercritical CO2 Power Cycles; Wind Energy, ASME; 2016, p. V009T36A004. doi:10.1115/GT2016-56459.

[27] Zhang J. The 6th International Supercritical CO2 Power Cycles Symposium Dynamic modeling and transient analysis of a molten salt heated recompression supercritical CO2 Brayton cycle. n.d.

[28] Luu MT, Milani D, McNaughton R, Abbas A. Dynamic modelling and start-up operation of a solar-assisted recompression supercritical CO2 Brayton power cycle. Applied Energy 2017;199:247–63. doi:10.1016/J.APENERGY.2017.04.073.

[29] Bianchi G, Saravi SS, Loeb R, Tsamos KM, Marchionni M, Leroux A. Design of a high-temperature heat to power conversion facility for testing supercritical CO2 equipment and packaged power units. Energy Procedia 2019;161:421–8. doi:10.1016/J.EGYPRO.2019.02.109.

[30] T Gamma - Gamma Technologies Inc 2012. GT-SUITE-Flow Theory Manual 2012.

[31] Lemmon, E. W., Marcia L. Huber and MOM. REFPROP, NIST Standard Reference Database 23, Version 8.0. 2007.

[32] Pitla SS, Groll EA, Ramadhyani S. New correlation to predict the heat transfer coefficient during in-tube cooling of turbulent supercritical CO2. International Journal of Refrigeration 2002;25:887–95. doi:10.1016/S0140-7007(01)00098-6.

[33] Cipollone R, Bianchi G, Di Battista D, Fatigati F. Experimental and numerical analyses on a plate heat exchanger with phase change for waste heat recovery at off-design conditions. Journal of Physics: Conference Series 2015;655:12038. doi:10.1088/1742-6596/655/1/012038.

[34] Colebrook CF, Blench T, Chatley H, Essex EH, Finnincome JR, Lacey G, et al. Turbulent flow in pipes, with particular reference to the transition region between the smooth and rough pipe laws. (include plates). Journal of the Institution of Civil Engineers 1939;12:393–422. doi:10.1680/ijoti.1939.14509.

[35] Marchionni M, Bianchi G, Karvountzis-Kontakiotis A, Pesyridis A, Tassou SA. An appraisal of proportional integral control strategies for small scale waste heat to power conversion units based on Organic Rankine Cycles. Energy 2018;163:1062–76. doi:10.1016/J.ENERGY.2018.08.156.

[36] Marchionni M, Bianchi G, Karvountzis-Kontakiotis A, Pesiridis A, Tassou SA. Dynamic modeling and optimization of an ORC unit equipped with plate heat exchangers and turbomachines. Energy Procedia 2017;129:224–31. doi:10.1016/J.EGYPRO.2017.09.146.

[37] Baltadjiev ND, Lettieri C, Spakovszky ZS. An Investigation of Real Gas Effects in Supercritical CO $_2$ Centrifugal Compressors. Journal of Turbomachinery 2015;137:91003. doi:10.1115/1.4029616.

DOI: 10.17185/duepublico/48908

DOI: 10.17185/duepublico/48908
URN: urn:nbn:de:hbz:464-20191004-145238-6